Origami Hexagon Deformations and Flip Graph

July 2020

Abstract

We studied the collection of configurations of an isolated hexagon consisting of six equilateral triangles around a vertex on the triangular lattice. We quantitatively characterized the moduli space of deformations near the flat state. The rational and integer points on the deformation surface joining with flip operations admit some consistent combinatorial structure.

Contents

1 Introduction

By utilizing origami folding processes, researchers have been able to solve a wide range of engineering problems such as fabricating different robot morphologies [1] and manufacturing folding-based mechanisms [7]. Leveraging origami structures with given crease patterns requires an understanding of geometric and numerical properties of folding configurations. An origami hexagon, as an undividable functional unit of the hexagonal lattice, is studied in this paper. We describe rational parametrizations of the angles. We discretize the configuration space by introducing a flip operation and therefore construct a flip graph to help understand the classifications of an origami hexagon.

Izmestiev reexamined the parametrization of the angles in a general four-bar linkage [8] with similar simplification techniques, which is regarded as a planar analogue of the study on an origami hexagon. A flip transformation for a planar quadrilateral is introduced in the Darboux' folding porism [6].

In Section 2, we review the moduli space of deformations near the flat state. In Section 3, we discuss the rational parametrization. In Section 4 and 5, we define flip operations and create a flip graph analogous to the Calkin–Wilf tree. In Section 6, the connection between Pythagorean 4-tuples and integer solutions is investigated.

2 Summary

2.1 An isolated origami hexagon

An isolated origami hexagon consists of six equilateral triangles around a vertex on the triangular lattice, as shown in Figure 1a. Only considering the region marked inside the blue boundary, Figure 1b indicates the crease pattern of an oriented isolated origami hexagon.

It is natural to ask what the relations among fold angles without curving subplanes or breaking hinges. We are interested in the configuration space of an oriented isolated origami hexagon, with each face being allowed to pass through itself. See more configuration examples in Figure 2. In the following context, every origami hexagon refers to an oriented isolated origami hexagon.

To understand the geometric classification problem for an origami hexagon, we parametrize its configuration collection by six fold angles,

$$(\theta_1, \theta_2, \cdots, \theta_6), \quad \theta_i \in \mathbb{R}/2\pi\mathbb{Z},$$

where each fold angle corresponds to a supplementary angle of a dihedral angle between two intersecting equilateral triangle planes affiliated with the hexagon, see Figure 1b. Note that θ_i is a supplementary angle, when two triangle faces overlap, the corresponding fold angle is close to π.

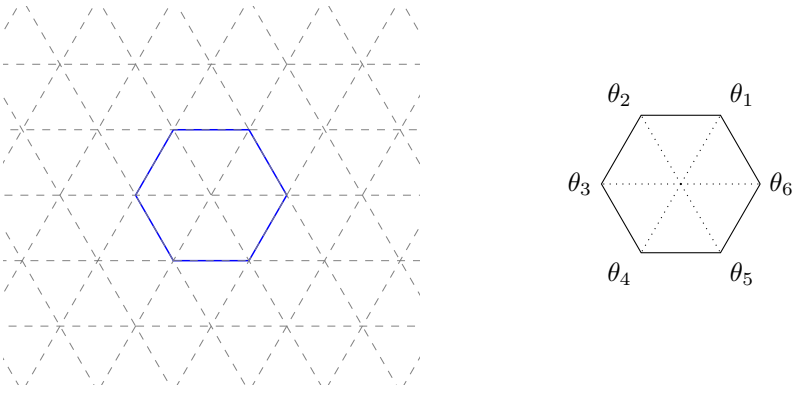

(a) Hexagon on triangular lattices (b) Isolated hexagon with parametrization

Figure 1: Origami hexagon

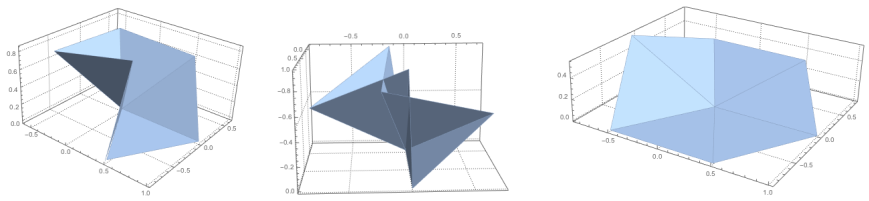

Figure 2: Hexagon configurations

The moduli space of the hexagon configuration collection is bounded by the hypercube $(\mathbb{R}/2\pi\mathbb{Z})^6$, with three degrees of freedom [5]. All origami hexagons belong to a three-parameter family.

2.2 Moduli space of deformations

In the context of **near flat configurations**, all the faces slightly deviate from one plane. Each dihedral angle between two adjacent triangle faces is close to π, thus each fold angle θ_i is small enough to apply Taylor expansion and second order approximation. The following calculation is in this quotient space

$$\mathbb{Q}[\theta_i]/(\theta_i^2, \theta_i\theta_j), \quad i \in \mathbb{Z}/6\mathbb{Z}, i \neq j.$$

Cut and glue We use "double counting" technique to characterize relations among fold angles. We cut the hexagon along some creases into two parts. To make a valid hexagon, when they are glued back, the corresponding distances should match.

(a) First cut (b) Second cut

Figure 3: Cut and glue

The first cut is cutting the hexagon in half, resulting in two 3-triangle halves as shown in Figure 3a. In $\mathbb{R}^3$, after folding the top half with angles θ_1, θ_2, and the bottom half with θ_4, θ_5, a valid configuration needs the angle between OA and OB equal to the angle between $O'A'$ and $O'B'$. Applying rotation transformations, the distance from A to B in $\mathbb{R}^3$ could be represented by $\mathbf{f}(\theta_1+\theta_2)$. Symmetrically, the distance from A' to B' is $\mathbf{f}(\theta_4+\theta_5)$ [5], which indicates

$$\theta_1 + \theta_2 = \theta_4 + \theta_5.$$

The second cut is cutting the hexagon into a 4-triangle one and a 2-triangle one as shown in Figure 3b. The distance between CD is $\mathbf{g}(\theta_2^2 + 2\theta_1\theta_2 + 2\theta_2\theta_3 + 2\theta_1\theta_3)$. The distance between $C'D'$ is $\mathbf{g}(\theta_5^2)$. Then

$$x_5^2 = x_2^2 + 2x_1x_2 + 2x_2x_3 + 2x_1x_3$$

There are three different axes of symmetry to cut a hexagon in half and three different dividing ways to choose in the second cut.

Combining all the relations fold angles have to satisfy, we obtain an algebraic variety Y in $\mathbb{R}^6$,

$$Y = \begin{cases} x_5^2 = x_2^2 + 2x_1x_2 + 2x_2x_3 + 2x_1x_3 \\ x_1 + x_2 = x_4 + x_5 \\ x_2 + x_3 = x_5 + x_6. \end{cases} \tag{1}$$

It's clear that Y is a necessary condition for the angle set of a near-flat hexagon. More importantly, Y is the precise description for all near-flat configurations. Each solution satisfying Y is a valid configuration and each near-flat hexagon's six fold angles is a 6-tuple point on Y.

Claim 1. *Algebraic variety Y is the moduli space of deformations of near-flat hexagon configurations.*

Proof. According to Chen and Santangelo, the space of deformations near the flat state is described by the null cone of some quadratic form [4]. For an origami hexagon, its moduli space has dimension 3 [5]. Thus we have such congruence,

$$\left\{\begin{array}{r}\text{Near-flat hexagon}\\ \text{configurations}\end{array}\right\} \cong \left\{\begin{array}{r}\text{Null cone of some quadratic}\\ \text{form } Q \text{ with dimension } 3\end{array}\right\} \tag{2}$$

Y is exactly described by the quadratic null cone inside $\mathbb{R}^4$ with actual dimension 3. We have shown that near-flat deformations are a subset of Variety Y. Then

$$\mathbb{R}^6 \supset V^4 \cong \mathbb{R}^4 \supset Y \cong \left\{\begin{array}{r}\text{Null cone of some quadratic}\\ \text{form } Q \text{ with dimension } 3\end{array}\right\} \tag{3}$$

Combining Eq (2) and Eq (3),

$$Y \cong \left\{\begin{array}{r}\text{Near-flat hexagon}\\ \text{configurations}\end{array}\right\},$$

we conclude that Y represents the moduli space of deformations near flat. □

Y has the same topological shape as the quadratic form

$$x_1^2 + x_2^2 + x_3^2 - x_4^2 = 0,$$

which has signature $(3, 1)$. Thus, Y's topological shape is described by a product of spheres, $S^2 \times S^0$.

Claim 2. *Y has the same topological shape as $\mathcal{C} : w^2 = y^2 + 2xy + 2yz + 2xz$.*

Proof. Y, as a subspace of $\mathbb{R}^6$, is a subspace of $\mathbb{R}^4$. The map sending $(x_1, \cdots, x_6)$ in Y to $(w = x_1, y = x_4, x = x_3, z = x_5)$ is a continuous bijection, and the inverse function is also continuous. So Y has the same topological shape as $w^2 = y^2 + 2xy + 2yz + 2xz$. □

In the following context, we would refer Y as the (near flat) hexagon configuration surface.

2.3 Mountain-valley classification

To help classify different configuration types, we introduce mountain-valley description. We call a fold *mountain* if the corresponding fold angle is positive; otherwise, *valley*. In graphs, we use a dotted line to represent a *valley* fold and a solid line to represent a *mountain* fold. See Figure 4.

(a) Mountain fold (b) Valley fold

Figure 4

For an origami hexagon, each fold could be a mountain, a valley or a facet crease (where the fold angle is zero). But we don't have 2^6 types of labelling in total since some mountain-valley crease pattern does not exist. All mountain-valley labellings for an unoriented origami hexagon are enumerated in Figure 5.

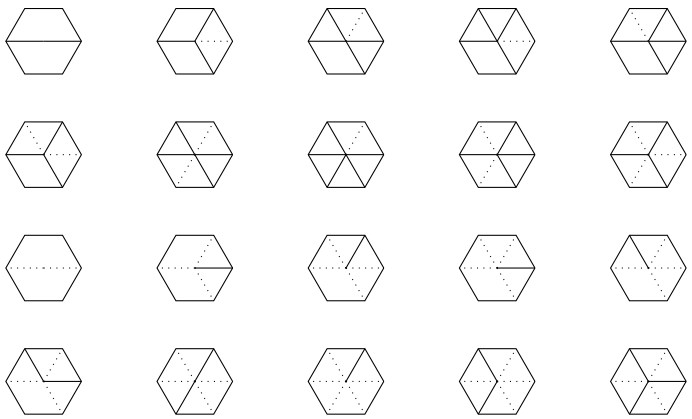

Figure 5: Mountain-valley labellings

3 Rational points on the hexagon surface

Rational solutions are representing the practical crease angles, where it is natural to correspond rational points on the hexagon surface to physical configurations.

To characterize rational solutions of quadratic equations with rational coefficients, a geometric idea is to parametrize a line intersecting with the quadratic surface. There are two intersection points by the fundamental theorem of algebra. Given a rational point O on a quadratic surface, we have such correspondence

$$\{\text{Rational lines through } O\} \cong \{\text{Rational intersection points on the surface}\}.$$

3.1 A quadratic surface

Before diving into the rational points on this hexagon configuration surface Y, we first examine the rational parametrization for a quadratic surface taking the form

$$w^2 = y^2 + 2xy + 2yz + 2xz,$$

denoted as $\mathcal{C}$.

Suppose O is a rational point on the surface $\mathcal{C}$. Each rational line through O intersects $\mathcal{C}$ with two rational points, O itself and another point P. Conversely, each rational point P on $\mathcal{C}$ could form a ration line by joining P to O. There is a one-to-one map from the coefficients of rational lines through O to all but one of the rational points on $\mathcal{C}$. The exceptional line is vertical to x-axis.

With the substitution $v = x + z - y$, the curve takes the form

$$w^2 + x^2 + z^2 = v^2.$$

When $v = 0$, $(x, y, z, w) = (0, 0, 0, 0)$.
When v is nonzero, it is equivalent to working in the affine space $\mathbb{R}^3$. With convenient notations

$$a = \frac{x}{v}, c = \frac{w}{v}, b = \frac{z}{v},$$

we obtain

$$a^2 + b^2 + c^2 = 1,$$

which passes through $(1, 0, 0)$.

Given rational variables r, s, and t, a rational line L passing through $(1, 0, 0)$ hash such the parametrization

$$L = \begin{cases} a - 1 = rm \\ b = sm \\ c = tm \end{cases}.$$

When $m = 0$, there is one solution $(a, b, c) = (1, 0, 0)$.
When $m \neq 0$, m could be simplified as

$$m = \frac{-2r}{s^2 + t^2 - r^2}.$$

Then (a, b, c) takes the form

$$a = rm + 1 = \frac{s^2 + t^2 - r^2}{s^2 + t^2 + r^2}$$
$$b = sm = \frac{-2sr}{s^2 + t^2 + r^2}$$
$$c = tm = \frac{-2tr}{s^2 + t^2 + r^2}.$$

Tracing back, taking v as $s^2 + t^2 + r^2$, (x, y, z, w) could be parametrized as

$$x = s^2 + t^2 - r^2$$
$$y = 2r^2 + 2tr$$
$$z = -2tr$$
$$w = -2sr.$$

In conclusion, there is a surjective map from all rational (s, t, r) tuples to all rational lines through $(1, 0, 0)$, as well as all rational points on the quadratic surface $w^2 = y^2 + 2xy + 2yz + 2xz$.

3.2 Rational parametrization

With the rational paremetrization of $w^2 = y^2 + 2xy + 2yz + 2xz$, we could deploy a surjective map from all the rational lines through one rational point on this hexagon surface, to all the other rational points . Consider a 6-tuple $\theta = (\theta_1, \theta_2, \cdots, \theta_6) \in \mathbb{R}^6$, satisfying

$$\theta_5^2 = \theta_2^2 + 2\theta_1\theta_2 + 2\theta_2\theta_3 + 2\theta_1\theta_3.$$

We have given out the rational parametrization for this quadratic form in Section 3.1 as

$$\theta_1 = x = s^2 + t^2 - r^2$$
$$\theta_2 = y = 2r^2 + 2tr$$
$$\theta_3 = z = -2tr$$
$$\theta_5 = w = -2sr.$$

With two more linear constraints in Y,

$$\theta_4 = \theta_1 + \theta_2 - \theta_5$$
$$\theta_6 = \theta_2 + \theta_3 - \theta_5,$$

we obtain the complete rational patametrization for a near-flat origami hexagon,

$$\theta_1 = s^2 + t^2 - r^2$$
$$\theta_2 = 2r^2 + 2tr$$
$$\theta_3 = -2tr$$
$$\theta_4 = s^2 + t^2 + 2tr + 2sr + r^2$$
$$\theta_5 = -2sr$$
$$\theta_6 = 2r^2 + 2sr.$$

All representations for θ_i's are rational functions of variables s, t, r. When $(s, t, r) \in \mathbb{Q}^3$, each (s, t, r) decides a rational line, which corresponds to a set of rational hexagon fold angles.

Theorem 1 (Real solutions)**.** *For each real six-tuple $\theta = (\theta_1, \theta_2, \cdots, \theta_6), \theta_i \in \mathbb{R}$ on the hexagon surface, there exists a sequence of rational six-tuples $\{R_n\}_{n\geq 1}$ satisfying Y that uniformly converges to θ.*

Proof. All the (s,t,r)-functions in $\mathbb{R}^3$ for θ are continuous. The rationals are a dense subset in $\mathbb{R}$, which indicates that for any real solution on the hexagon surface, we could find a rational solution sequence arbitrarily close to it. □

4 Complexity and flip operation

4.1 Complexity

A noteworthy character for the set of real hexagon configurations with the form

$$(\theta_1, \theta_2, \cdots, \theta_6) \in \mathbb{R}^6$$

is that there doesn't exist any non-flat 6-tuple with the sum of angles zero, i.e. $\sum_i \theta_i = 0$. A hexagon configuration is flat if all fold angles are zero. We would prove this later in Proposition 5.

The sum of six fold angles is such an important character for a configuration that it deserves a name, ***complexity***. We classify real configurations by the sign of $\sum \theta_i$.

Definition 1 (Complexity)**.** *A real hexagon configuration $(\theta_1, \theta_2, \cdots, \theta_6) \in \mathbb{R}^6$ has a positive complexity if $\sum \theta_i > 0$; otherwise, a negative complexity.*

There are some properties regarding to the partial sum of fold angles. All the subscripts are in $\mathbb{Z}/6\mathbb{Z}$.

Proposition 1. *Suppose $(\theta_1, \theta_2, \cdots, \theta_6)$ is a valid real configuration with a positive complexity, $\sum \theta_i > 0$, then*

(a). $\theta_i + \theta_{i+1} \geq 0$

(b). $\theta_{i-1} + \theta_i + \theta_{i+1} > 0$

(c). $\theta_{i-1} + \theta_i + \theta_{i+1} \geq -2\theta_i$

Proof. We will prove the second statement first.

(b). If there exists three consecutive angles with a nonpositive sum, without loss of generality, suppose $\theta_1 + \theta_2 + \theta_3 \leq 0$. Since $(\theta_1, \theta_2, \cdots, \theta_6)$ satisfies Y, we have

$$\theta_5^2 = \theta_2^2 + 2\theta_1\theta_2 + 2\theta_2\theta_3 + 2\theta_1\theta_3 \tag{4}$$

Adding $\theta_1^2 + \theta_3^2$ on both sides of Eq (4), it takes the form

$$\theta_1^2 + \theta_3^2 + \theta_5^2 = (\theta_1 + \theta_2 + \theta_3)^2 \tag{5}$$

When $\theta_1 + \theta_2 + \theta_3 \leq 0$,

$$\theta_1 + \theta_2 + \theta_3 = \theta_3 + \theta_4 + \theta_5 = \theta_5 + \theta_6 + \theta_1 = -\sqrt{\theta_1^2 + \theta_3^2 + \theta_5^2}$$

Summing up $\theta_1 + \theta_2 + \theta_3$, $\theta_3 + \theta_4 + \theta_5$, and $\theta_5 + \theta_6 + \theta_1$, we add the rightmost term three times,

$$\sum \theta_i = -3\sqrt{\theta_1^2 + \theta_3^2 + \theta_5^2} - (\theta_1 + \theta_3 + \theta_5)$$

Since $a^2 + b^2 + c^2 \geq (a+b+c)^2/3$, we have the summation of all angles nonpositive,

$$9(\theta_1^2 + \theta_3^2 + \theta_5^2) \geq (\theta_1 + \theta_3 + \theta_5)^2 \;\Rightarrow\; \sum \theta_i \leq 0,$$

which contradicts to the assumption. Thus $\theta_i + \theta_{i+1} + \theta_{i+2} > 0$, for any θ_i.

(a). Back to the first claim. If $\theta_i + \theta_{i+1} < 0$, without loss of generality, suppose $\theta_1 + \theta_2 < 0$, we have

$$\theta_1 + \theta_2 + \theta_3 = \pm\sqrt{\theta_1^2 + \theta_3^2 + \theta_5^2}.$$

Since we have proved that $\theta_1 + \theta_2 + \theta_3 > 0$,

$$\theta_1 + \theta_2 = \sqrt{\theta_1^2 + \theta_3^2 + \theta_5^2} - \theta_3 < 0$$

$$\Leftrightarrow \quad \sqrt{\theta_1^2 + \theta_3^2 + \theta_5^2} < \theta_3 \quad \Leftrightarrow \quad \theta_1^2 + \theta_5^2 < 0,$$

which is a contradiction. Thus, $\theta_i + \theta_{i+1} \geq 0$.

(c). Without loss of generality, we could only check the case for $\theta_2 + 2\theta_3 + \theta_4 \geq -\theta_3$. Based on (b) and $a^2 + b^2 + c^2 \geq (a + b + c)^2/3$, we obtain

$$(\theta_1 + \theta_2 + \theta_3) + (\theta_3 + \theta_4 + \theta_5) = 2\sqrt{\theta_1^2 + \theta_3^2 + \theta_5^2} \geq \frac{2}{\sqrt{3}}(\theta_1 + \theta_3 + \theta_5) \geq \theta_1 + \theta_5 - \theta_3$$

$$\Leftrightarrow \quad (\theta_2 + 2\theta_3 + \theta_4) + \theta_1 + \theta_5 \geq \theta_1 + \theta_5 - \theta_3$$

$$\Leftrightarrow \quad \theta_2 + 2\theta_3 + \theta_4 \geq -\theta_3.$$

□

Notice that symmetrically, if $\sum \theta_i < 0$, we have $\theta_i + \theta_{i+1} \leq 0$ and $\theta_i + \theta_{i+!} + \theta_{i+2} < 0$.

Now, we could complete the proof of the nonexistence of any non-flat configuration with zero complexity.

Proposition 2. *Any non-flat real* 6*-tuple* $(\theta_1, \theta_2, \cdots, \theta_6)$ *satisfying* Y *has* $\sum_i \theta_i$ *either positive or negative.*

Proof. By Equation (5), if $\sum \theta_i = 0$,

$$9(\theta_1^2 + \theta_3^2 + \theta_5^2) = (\theta_1 + \theta_3 + \theta_5)^2$$

The equality only holds when $\theta_1 = \theta_3 = \theta_5 = 0$, but this will lead to an all-zero solution, contradiction. □

4.2 Flip operation

Observation 2. *If* $(x, y, z) \in \mathbb{R}^3$ *satisfies*

$$0 = Q(x, y, z) = y^2 + 2xy + 2xz + 2yz = 0,$$

then

$$0 = Q(2y + x, -y, 2y + z).$$

Points on the hexagon surface has the same transition invariant above. When we turn one mountain crease to a valley one with the same fold angle value, and add some specific values to its neighbors, the new point could still remain on this hexagon surface.

We call this inter-set transformation the *flip operation*. There are six natural *flip operations* on the space Y, corresponding to a local change at each of those six folds on the hexagon.

Definition 2 (Flip)**.** *A* ***flip operation*** *applied on a fold, with angle* θ_i *is a function*

$$F_i : \mathbb{R}^6 \to \mathbb{R}^6,$$

such that

$$\begin{aligned}\theta_{i-1} &\to \theta_{i-1} + 2\theta_i \\ \theta_{i+1} &\to \theta_{i+1} + \theta_i \\ \theta_i &\to -\theta_i\end{aligned}$$

The other angles remain the same, i.e.,

$$F_i(\theta_1, \theta_2, \cdots, \theta_6) = (\cdots, \theta_{i-1} + 2\theta_i, -\theta_i, \theta_{i+1} + 2\theta_i, \cdots)$$

In the vector space $\mathbb{R}^6$, F_i is a linear map with matrix M_i,

$$\begin{pmatrix} 1 & & & & & & \\ & \ddots & & & & & \\ & & 1 & 2 & & & \\ & & & -1 & & & \\ & & & 2 & 1 & & \\ & & & & & \ddots & \\ & & & & & & 1 \end{pmatrix}$$

For example, F_2 acts on configurations as shown in Figure 6.

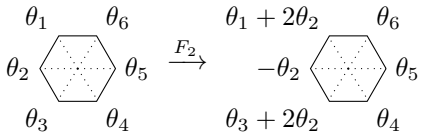

Figure 6: Flip operation

Note that the inverse of F_i has the same matrix as M_i, thus ${F_i}^2 = Id$.

Proposition 3. *Suppose two six-tuples θ, γ are connected by a flip operation F_i, i.e. $F_i(\theta) = \gamma$. If θ is a valid hexagon configuration, i.e. satisfying variety Y, then γ satisfies Y.*

Proof. This is directly deduced by Observation 2 and Claim 1. Without loss of generality, we suppose a flip operation F_2 is applied on $\theta = (\theta_1, \theta_2, \cdots, \theta_6)$. Then the new six-tuple γ is

$$(\gamma_1 = \theta_1 + 2\theta_2, \gamma_2 = -\theta_2, \gamma_3 = \theta_3 + 2\theta_2, \gamma_4 = \theta_4, \gamma_5 = \theta_5, \gamma_6 = \theta_6).$$

Considering θ satisfies the variety Y,

$$\begin{aligned}\gamma_1 + \gamma_2 &= \theta_1 + 2\theta_2 - \theta_2 = \theta_1 + \theta_2 = \theta_4 + \theta_5 = \gamma_4 + \gamma_5 \\ \gamma_2 + \gamma_3 &= -\theta_2 + \theta_3 + 2\theta_2 = \theta_2 + \theta_3 = \theta_5 + \theta_6 = \gamma_5 + \gamma_6 \\ \gamma_2^2 + 2\gamma_1\gamma_2 + 2\gamma_2\gamma_3 + 2\gamma_1\gamma_3 &= \theta_2^2 - 2(\theta_1 + 2\theta_2)\theta_2 - 2\theta_2(\theta_3 + 2\theta_2) + 2(\theta_1 + 2\theta_2)(\theta_3 + 2\theta_2) \\ &= \theta_2^2 + 2\theta_1\theta_2 + 2\theta_2\theta_3 + 2\theta_1\theta_3 = \theta_5^2 = \gamma_5^2\end{aligned}$$

The γ satisfies the variety Y. □

Combining complexity and flip, an interesting observation is that the sign of the complexity would be preserved under flip operations.

Proposition 4. *For any two real hexagon configurations connected by a flip operation described in Definition 2,*

$$(\theta_1, \theta_2, \cdots, \theta_6) \xrightarrow{F_j} (\theta_1', \theta_2', \cdots, \theta_6').$$

(a) $\sum \theta_i' = (\sum \theta_i) + 2\theta_j$.

(b) If $\sum \theta_i > 0$, *then* $\sum \theta_i' > 0$. *Similarly, if* $\sum \theta_i < 0$, *then* $\sum \theta_i' < 0$.

(c) $\theta_i \equiv \theta_i' \mod 2$, *if* $(\theta_1, \theta_2, \cdots, \theta_6) \in \mathbb{Z}^6$.

Proof. (a). Flipping angle θ_j, we have the transformation

$$\begin{aligned} \theta_{j-1}' &= \theta_{j-1} + 2\theta_j \\ \theta_j' &= -\theta_j \\ \theta_{j+1}' &= \theta_{j+1} + 2\theta_j \end{aligned}$$

Then

$$\begin{aligned} \sum_i \theta_i' &= (\theta_{j-1} + 2\theta_j) + (-\theta_j) + (\theta_{j+1} + 2\theta_j) + \theta_{j+2} + \theta_{j+3} + \theta_{j+4} \\ &= \sum_j \theta_j + 2\theta_j = \sum_i \theta_i + 2\theta_j. \end{aligned}$$

(b). We only need to consider the case when $\sum \theta_i > 0$.

$$\sum \theta_i' = (\sum \theta_i) + 2\theta_j = (\theta_{j-1} + 3\theta_j + \theta_{j+1}) + (\theta_{j+2} + \theta_{j+3} + \theta_{j+4})$$

By Proposition 1(b), $\theta_{j+2} + \theta_{j+3} + \theta_{j+4} > 0$, and by Proposition 1(c), $\theta_{j-1} + 3\theta_j + \theta_{j+1} \geq 0$, thus,

$$\sum \theta_i' > 0.$$

(c). For the congruence classes mod 2,

$$\theta_{j-1}' \equiv \theta_{j-1} + 2\theta_j \equiv \theta_{j-1} \mod 2,$$

where the case is identical for θ_{j+1}.

$$\theta_j' = -\theta_j \equiv \theta_j \mod 2.$$

□

5 Integer points and the flip graph

Given any 6-tuple in $\mathbb{R}^6$ satisfying the hexagon surface, we could always fabricate such a hexagon with specified fold angles. The set of real solutions measures near-flat configurations physically.

To intuitively reflect the internal relations of near-flat configurations, such as how different configurations are transformed, how two hexagons could be described as "homogeneous", and what is left when real fold angles are scaled off, we change gear to integer points on the hexagon surface.

In the following context, we work on the primitive integer six-tuple $(\theta_1, \theta_2, \cdots, \theta_6)$, satisfying Y,

$$\theta_5^2 = \theta_2^2 + 2\theta_1\theta_2 + 2\theta_2\theta_3 + 2\theta_1\theta_3 \tag{6}$$

$$\theta_1 + \theta_2 = \theta_4 + \theta_5 \tag{7}$$

$$\theta_2 + \theta_3 = \theta_5 + \theta_6. \tag{8}$$

with $gcd(\theta_1, \theta_2, \cdots, \theta_6) = 1$.

Recall the flip operation we defined in Section 4.2.

5.1 Flip graph

Creating graphs could provide a structural way to study a group. The Calkin-Wilf tree is an inspiring example to order and recount rational numbers.

5.1.1 The Calkin-Wilf tree

Definition 3 (Calkin–Wilf Tree)**.** *The Calkin-Wilf tree is rooted at integer* 1*, and any rational number expressed in simplest terms as the fraction* $\frac{a}{b}$ *has as its two children the numbers* $\frac{a}{a+b}$ *and* $\frac{a+b}{b}$*.*

As shown in Figure 7, the Calkin-Wilf is determined by a root and a children generating rule.

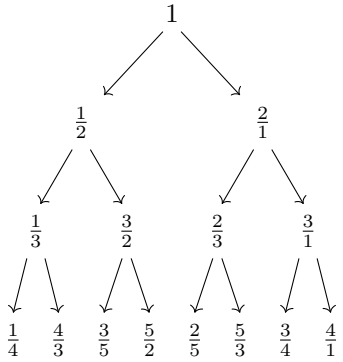

Figure 7: The Calkin-Wilf Tree

The fascinating property of the Calkin-Wilf tree is

Every positive rational number appears exactly once in the tree.[2]

5.1.2 Construct the flip graph

Analogous to the Calkin-Wilf tree, we defined the *flip graph* $\mathcal{G}$ with restricted flip operations.

Definition 4 (Flip graph)**.** *The flip graph* $\mathcal{G}$ *is constructed as follows:*

1. $\mathcal{G}$ *is rooted at primitive integer configurations where non-flat angles must be all positive or all negative. Then any valid root is one of three rotations of* $(0,0,1,0,0,1)$ *or one of three rotations of* $(0,0,-1,0,0,-1)$*.*

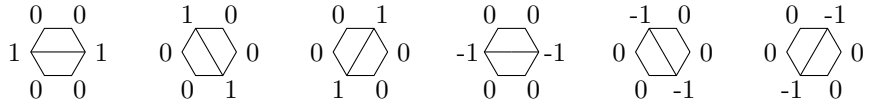

Figure 8: Roots for Flip Graph G

2. *A primitive integer configuration* $\theta = (\theta_1, \theta_2, \cdots, \theta_6) \in \mathbb{Z}^6$*, which is represented as a vertex in* $\mathcal{G}$*, has its children generated by flip operations with the following restrictions:*
   (a) *when* $\sum \theta_i > 0$*, the children of* θ *are* $\{F_i(\theta) |$ *for any* $\theta_i > 0\}$*,*
   (b) *when* $\sum \theta_i < 0$*, the children of* θ *are* $\{F_i(\theta) |$ *for any* $\theta_i < 0\}$*.*

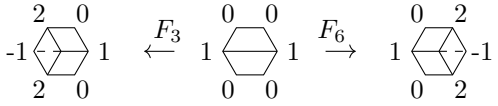

Figure 9: Children generating rule

In Figure 9, for example, suppose $\theta = (\theta_1 = 0, \theta_2 = 0, \theta_3 = 1, \theta_4 = 0, \theta_5 = 0, \theta_6 = 1)$. Then all the children θ has are $(0, 2, -1, 2, 0, 0, 1)$ generated by applying F_3 and $(2, 0, 1, 0, 2, -1)$ generated by applying F_6.

With roots defined and children generating rule specified, the flip graph is uniquely determined. Figure 10 shows the first three layers of one component in the flip graph $\mathcal{G}$ rooted with $(\theta_1, \theta_2, \cdots, \theta_6) = (0, 0, 1, 0, 0, 1)$.

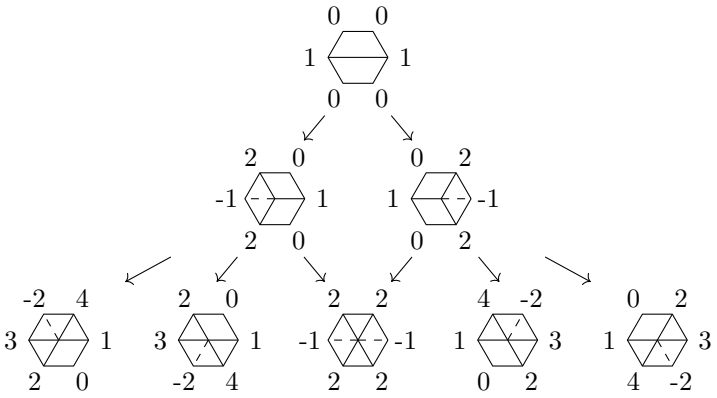

Figure 10: One component of flip graph $\mathcal{G}$, rooted with $(0, 0, 1, 0, 0, 1)$

5.1.3 Properties of the flip graph

From now on, we will be working with the flip graph $\mathcal{G}$. All flip operations we refer to would be restricted to Definition 4 instead of Definition 2, i.e. the valid flip operation could only be applied to positive angles when the hexagon complexity is positive, vice versa.

Claim 3. *Each vertex in the flip graph $\mathcal{G}$ corresponds to a valid primitive integer configuration of an origami hexagon.*

Proof. In $\mathcal{G}$, by definition, every root is a valid primitive integer configuration. All vertices are connected by a sequence of flip operations starting from a root. By Proposition 3, every vertex in $\mathcal{G}$ must be a valid configuration on the hexagon surface.

For primitiveness, the flip operation F_i and its inverse F_i^{-1} are associated with the same integer matrix M_i, which preserves common factors of six fold angle values. Therefore, any common angle value factor in $\mathcal{G}$ should exist in the root. Thus, the configuration corresponding to each vertex is primitive and integral. □

Claim 3 shows that there is an injective map from vertices in the flip graph $\mathcal{G}$ to primitive integer configurations. Every vertex is meaningful. Then we care about how many configurations this flip graph $\mathcal{G}$ could cover. Now, it is time to explore how the flip graph generates new points.

Flip operations defined in $\mathcal{G}$ has symmetry. Then we could only focus on flip operations on positive complexities. For a parent vertex in $\mathcal{G}$, the absolute values of its children's fold angles are non-decreasing.

Proposition 5. *In the flip graph $\mathcal{G}$, suppose $P = (\theta_1, \cdots, \theta_6)$ is a valid primitive integer configuration with $\sum \theta_i > 0$. It has a child $C = (\theta_1', \cdots, \theta_6')$ by flipping positive fold angle θ_j. Then*

(a). $|\theta_i'| \geq |\theta_i|$.

(b). $|\theta_{j+1}'| \geq |\theta_j|, |\theta_{j-1}'| \geq |\theta_j|$.

(c). θ_j *is unique, i.e. there does not exist any integer* k *such that* $F_k(P) = C, k \neq j$.

Proof. (a). We only need to check θ'_{j+1}. By Proposition 1(a), $\theta_j + \theta_{j+1} \geq 0$. Since a flip operation is acting on the positive angle, $\theta_j > 0$. Then by $|a+b| = |a| + |b|$, when $a, b > 0$,

$$|\theta'_{j+1}| = |\theta_{j+1} + 2\theta_j| = |\theta_{j+1} + \theta_j| + |\theta_j| \geq |(\theta_{j+1} + \theta_j) - \theta_j| = |\theta_j|.$$

(b). It is sufficient to check θ'_{j+1} only. With the same reason above, $\theta_j + \theta_{j+1} > 0, \theta_j > 0$, we have

$$|\theta'_{j+1}| = |\theta_{j+1} + 2\theta_j| = |\theta_{j+1} + \theta_j| + |\theta_j| \geq |(\theta_j|.$$

(c). Prove by contradiction. Suppose there exists k satisfying the above condition. Then in P, $\theta_k > 0$ and in C, $\theta'_k < 0$. However, C is generated by flipping θ_j on P, which could not make any angle positive except θ'_j. It is contradicted to the transition from a positive θ_k to a negative θ'_k. □

Claim 4. *The flip graph $\mathcal{G}$ consists of six isomorphic components.*

Proof. When $\sum \theta_i > 0$, the flip operation is defined on a positive angle $\theta_j > 0$. According to Proposition 4(a),

$$\sum \theta'_i = (\sum \theta_i) + 2\theta_j > 0$$

Then all configurations generated from the a root with positive complexity must remain in positive complexities. The same situation applies to roots with negative complexities. Then each vertex in $\mathcal{G}$ connected to a positive root cannot have a path to any negative root.

From Proposition 5(b), the angles' parity are the same if two vertices are connected, which shows every vertex connected to the root $(0, 0, 1, 0, 0, 1)$ is not connected to $(0, 1, 0, 0, 1, 0)$, as well as $(1, 0, 0, 1, 0, 0)$. Thus, there are three components rooted from each positive root respectively.

In conclusion, each root in Figure 8 is in a component of $\mathcal{G}$. All six roots are in different components isolated to each other. Since those roots are isomorphic to each other, the rest of the subgraph connected by flip operations in $\mathcal{G}$ makes six components isomorphic. □

Since six components are isomorphic, it is sufficient to study one piece, which is rooted at $(0, 0, 1, 0, 0, 1)$, denoted as graph $\mathcal{D}$.

Claim 5. *Graph $\mathcal{D}$ has the following properties:*

(a) D is acyclic.

(b) D is graded.

Proof. (a). Each flip would increase the complexity, so there is no flip operation sequence that could visit a configuration twice. So $\mathcal{D}$ has no directed cycle.

(b). The distance from one vertex to the root is consistent for different generating paths. □

To make the flip graph $\mathcal{G}$ capable of revealing the structure of primitive integer configurations, we are interested in the correspondence between primitive integer configurations and vertices in $\mathcal{G}$. Like how the Calkin-Wilf tree behaved, we expect the flip graph $\mathcal{G}$ performances similarly – containing a one-to-one correspondence between vertices and configurations.

With those angles sum properties in Proposition 1, we could prove that each primitive integer configuration must show up in the flip graph $\mathcal{G}$. Equivalently, each primitive integer configuration is reached by a root in Figure 8 through a sequence of valid flip operations.

Claim 6. *In the flip graph $\mathcal{G}$, every integer configuration $(\theta_1, \theta_2, \cdots, \theta_6)$ with $\sum \theta_i > 0$ and $gcd(\theta_1, \theta_2, \cdots, \theta_6) = 1$, is reached by one of the positive roots, i.e. three rotations of $(0, 0, 1, 0, 0, 1)$.*

Proof. Consider any primitive integer configuration θ with a positive complexity. All the possible mountain-valley labellings for a valid hexagon are exhaustive, as shown in Figure 5 [5].

If θ is a root, then it is in the flip graph $\mathcal{G}$.

If θ is not a root, then it must have a negative angle. Recursively apply the inverse of flip operation on $\theta's$ negative angles. There are two possibilities for the generation pattern:

a. θ generates a finite path with the end point as one of three rotations of $(0, 0, 1, 0, 0, 1)$,

b. θ generates an infinite path – visit infinite primitive integer configurations (consider repetitive visit)

If the path generated by reversed flip operations is finite, consider the last primitive integer configuration γ on this path. If γ is a root, it falls under Case a. If γ is not a root, then it must have a negative angle which could reach a new primitive integer configuration. This contradicts γ being the last one on this path.

By Proposition 1(c), a flip operation would preserve the sign of complexity. An inverse of the flip operation has the same property. Here inverse of flip operations are recursively applied on negative angles, so the complexity is progressively decreasing. In that case the path could not revisit any configuration nor form an infinite path. Case b is impossible when applying reversed flip operations on negative angles.

Now, the only possible case left is Case a. For any integer primitive configuration we could find a finite path from itself to one of the roots by recursively applying the inverse of flip operation on negative angles. Reverse the direction of this path. Each integer primitive configuration must be reached by one of the roots through a sequence of flip operations applying on positive angles, which is exactly what we defined in the flip graph $\mathcal{G}$. □

Now, we reach an analogue to the Calkin-Wilf tree.

Theorem 3 (The bijective map)**.** *Primitive integer configurations on the hexagon surface correspond one-to-one to the vertices in the flip graph $\mathcal{G}$.*

Proof. By Claim 3, we have an injective map from vertices to primitive integer configurations. Claim 6 indicates the map is surjective. □

5.2 Mountain-valley distribution

After one subsection's effort of showing the existance of a bijective map, we could leverage this map to calculate the limiting distribution for mountain-valley configurations.

5.2.1 Limiting distribution

According to Proposition 1 and Theorem 3, configurations with positive complexity could not contain two consecutive negative fold angles. They must have the following configurations in Figure 11 up to rotations.

Here we have mountain-valley types with different degrees of freedom. Type A and B have one degree of freedom, then we use 0-dimensional to describe them. Type BB_2, BA, AB, AA have one degree of freedom, thus they are 1-dimensional configurations. Type BB_3, AAB, ABB, AAA have two degree of freedom. They are 2-dimensional configurations.

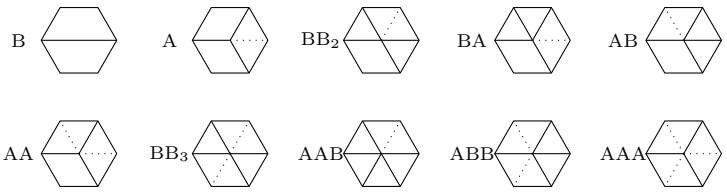

Figure 11: Mountain-valley labellings with positive complexity

Given a mountain-valley type, its children in the flip graph $\mathcal{G}$ are determined, as shown in Figure 12. Keep generating children recursively. The dominant types will be those 2-dimensional ones, BB_3, AAB, ABB, AAA. The state transition diagram is shown in Figure 13. Based on the mountain-valley transition relations, in the perspective of Markov transition process, the column-stochastic

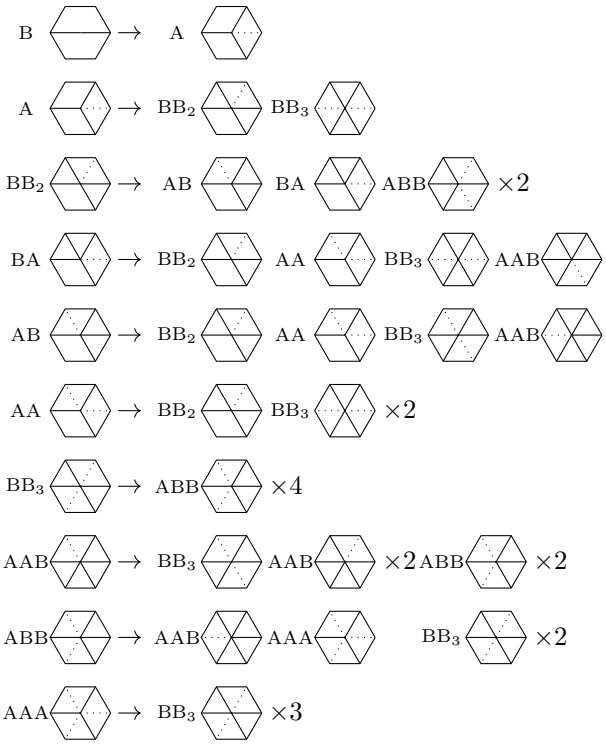

Figure 12: Flip images of configurations with positive complexity

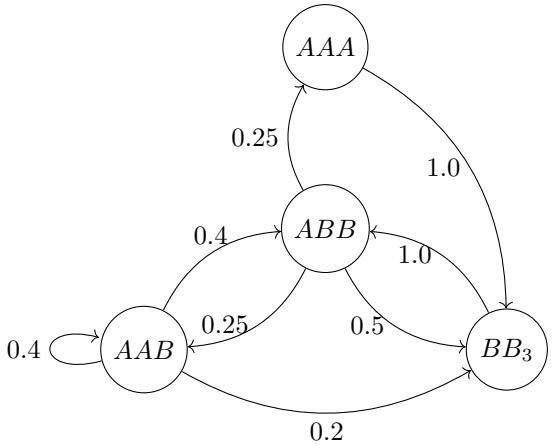

Figure 13: State transition diagram for 2-dimensional types BB_3, AAB, ABB, AAA

transition matrix for 2-dimensional configurations BB_3, AAB, ABB, AAA is

$$\begin{array}{c|cccc} & BB_3 & AAB & ABB & AAA \\ BB_3 & 0 & 0.2 & 0.5 & 1.0 \\ AAB & 0 & 0.4 & 0.25 & 0 \\ ABB & 1.0 & 0.4 & 0 & 0 \\ AAA & 0 & 0 & 0.25 & 0 \end{array},$$

with eigenvector $v = \begin{pmatrix} 1/3 \\ 1/6 \\ 2/5 \\ 1/10 \end{pmatrix}$ corresponding to the dominant eigenvalue $\lambda = 1$. Thus the final

distribution for those mountain-valley configurations is consistent with v.

Claim 7. *The limiting distribution for BB_3, AAB, ABB, AAA is*

$$BB_3 : AAB : ABB : AAA = \frac{1}{3} : \frac{1}{6} : \frac{2}{5} : \frac{1}{10} = 0.33 : 0.17 : 0.4 : 0.1.$$

Note: the limit ratio for $0,1$-dimensional configurations is 0.

5.2.2 Layer counting

Consider the isolated component $\mathcal{D}$ with root $(1,0,0,1,0,0)$. Recall Claim 5, Graph $\mathcal{D}$ is graded. As a result, we could classify vertices in $\mathcal{D}$ by layers, where

$$\{\text{nodes on Layer } n^{th}\} := \{\text{nodes which need } n \text{ flips to reach a root node}\}.$$

Mountain-valley configuration is a good tool to help classifying vertices on D. We have discussed how flip operation works on mountain-valley configurations. Since D is determined by the root and flip operations, we could calculate the number of nodes on each layer by discussing different mountain-valley configurations separately.

In the following context, we will focus on 2-dimensional configurations BB_3, AAB, ABB, AAA on each layer.

Proposition 6. *Each configuration in $\mathcal{D}$ has k parents, where k is the number of negative fold angles it has.*

Proof. Consider a configuration C in $\mathcal{D}$, we apply the inverse of flip operation on a negative angle to generate another vertex in $\mathcal{D}$, denoted by P. By how we defined parent-child relationship in Definition 4, P must be a valid parent for C. Most importantly, according to Proposition 5(c), all the parents of C would not overlap. Thus the number of negative angles in C indicates the number of parents it has in graph $\mathcal{D}$. □

To go from Layer n^{th} to Layer $(n+1)^{st}$, the number of children is determined by a node's mountain-valley type. For example, a node with AAB type has 5 positive angles to fold. Two of them will generate two children in type AAB as well. The other two will generate 2 children in type ABB. The left one will generate 1 child in type BB_3. Also, some children are counted multiple times, because they have more than one parents. For example, ABB has 2 negative folds, which indicates it is counted as a child twice.

Figure 14 shows the transitions among 2-dimensional types. The blue arrow means how many parents a type could have. A black arrow from type a to type b with number x means a generates x children in b type.

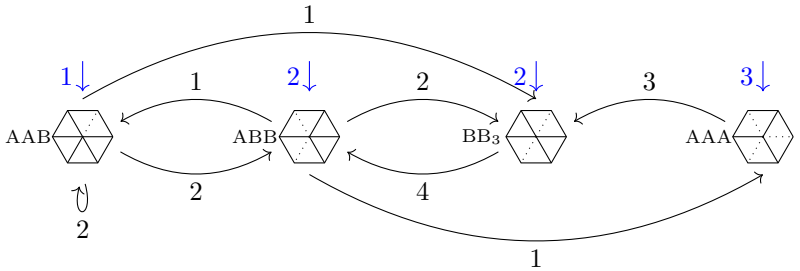

Figure 14: Transitions among 2-dimensional configurations

Let

$$type(n) = \#\{\text{nodes in configuration } type \text{ on Layer } n^{th}\}, \text{where } type = BB_3, AAB, ABB, or AAA.$$

According to the child-parent relation, the vector of numbers of nodes on Layer $(n+1)^{st}$ is the one on the previous layer timed with the transition matrix, respectively divided by the number of parents.

$$\begin{pmatrix} 2\cdot BB_3(n+1) \\ AAB(n+1) \\ 2\cdot ABB(n+1) \\ 3\cdot AAA(n+1) \end{pmatrix} = \begin{pmatrix} 0 & 1 & 2 & 3 \\ 0 & 2 & 1 & 0 \\ 4 & 2 & 0 & 0 \\ 0 & 0 & 1 & 0 \end{pmatrix} \begin{pmatrix} BB_3(n) \\ AAB(n) \\ ABB(n) \\ AAA(n) \end{pmatrix}$$

$$\Rightarrow \begin{pmatrix} BB_3(n+1) \\ AAB(n+1) \\ ABB(n+1) \\ AAA(n+1) \end{pmatrix} = \begin{pmatrix} 0 & 1/2 & 1 & 3/2 \\ 0 & 2 & 1 & 0 \\ 2 & 1 & 0 & 0 \\ 0 & 0 & 1/3 & 0 \end{pmatrix} \begin{pmatrix} BB_3(n) \\ AAB(n) \\ ABB(n) \\ AAA(n) \end{pmatrix}$$

Now, we have precisely described the growth trend for 2-dimensional configurations.

Claim 8. *The layer-counting transition matrix for 2-dimensional configurations is*

$$\begin{pmatrix} 0 & 1/2 & 1 & 3/2 \\ 0 & 2 & 1 & 0 \\ 2 & 1 & 0 & 0 \\ 0 & 0 & 1/3 & 0 \end{pmatrix}.$$

More generally, if we consider all the mountain-valley types in Figure 11, we have the layer-counting transition matrix H as

$$H = \begin{pmatrix} 0 & 0 & 0 & 0 & 0 & 0 & 0 & 0 & 0 & 0 \\ 1 & 0 & 0 & 0 & 0 & 0 & 0 & 0 & 0 & 0 \\ 0 & 1 & 0 & 1 & 1 & 1 & 0 & 0 & 0 & 0 \\ 0 & 0 & 1 & 0 & 0 & 0 & 0 & 0 & 0 & 0 \\ 0 & 0 & 1 & 0 & 0 & 0 & 0 & 0 & 0 & 0 \\ 0 & 0 & 0 & 1 & 1 & 0 & 0 & 0 & 0 & 0 \\ 0 & 1/2 & 0 & 1/2 & 1/2 & 1 & 0 & 1/2 & 1 & 3/2 \\ 0 & 0 & 0 & 1 & 1 & 0 & 0 & 2 & 1 & 0 \\ 0 & 0 & 1 & 0 & 0 & 0 & 2 & 1 & 0 & 0 \\ 0 & 0 & 0 & 0 & 0 & 0 & 0 & 0 & 1/3 & 0 \end{pmatrix}$$

With H specified, the number of nodes on each layer is determined.

Proposition 7. *The number of nodes on each layer has growing speed $O(t^n)$, where t is the dominant eigenvalue for H, $t = 1+\sqrt{3}$.*

6 Pythagorean 4-tuples

In the proof of Proposition 1, an equivalent representation for the quadratic equation in Y is noteworthy:

$$x_1^2 + x_3^2 + x_5^2 = (x_1 + x_2 + x_3)^2$$

If we set $r = x_1 + x_2 + x_3$, then (x_1, x_3, x_5, r) satisfying $x_1^2 + x_3^2 + x_5^2 = r^2$ uniquely determines a valid hexagon configuration $(\theta_1, \theta_2, \cdots, \theta_6)$ by taking the form

$$\begin{aligned} \theta_1 &= x_1 \\ \theta_3 &= x_3 \\ \theta_5 &= x_5 \\ \theta_2 &= r - x_1 - x_3 \\ \theta_4 &= r - x_3 - x_5 \\ \theta_6 &= r - x_1 - x_5. \end{aligned}$$

When we study primitive integer configurations, Pythagorean 4-tuples should be gazed.

Definition 5 (Pythagorean 4-tuples)**.** (x_1, x_2, x_3, x_4) *is a* ***primitive Pythagorean 4-tuple*** *if* x_1, x_2, x_3, x_4 *are integers satisfying*

$$x_1^2 + x_2^2 + x_3^2 = x_4^2, \qquad \gcd(x_1, x_2, x_3, x_4) = 1, \qquad \textit{and} \qquad x_4 > 0.$$

6.1 Transformations on Pythagorean 4-tuples

According to Cass and Arpaia [3], on Pythagorean 4-tuples, there is an action characterized by the composition of sign changes and the matrix A_4

$$A_4 = \begin{pmatrix} 0 & -1 & -1 & 1 \\ -1 & 0 & -1 & 1 \\ -1 & -1 & 0 & 1 \\ -1 & -1 & -1 & 2 \end{pmatrix},$$

which generates other complicated Pythagorean 4-tuples from simpler ones.

For example, A_4 could send a primitive Pythagorean 4-tuple $(3, -2, -6, 7)$ to $(15, 10, 6, 19)$, which is also a primitive Pythagorean 4-tuple.

$$\begin{pmatrix} 0 & -1 & -1 & 1 \\ -1 & 0 & -1 & 1 \\ -1 & -1 & 0 & 1 \\ -1 & -1 & -1 & 2 \end{pmatrix} \begin{pmatrix} 3 \\ -2 \\ -6 \\ 7 \end{pmatrix} = \begin{pmatrix} 15 \\ 10 \\ 6 \\ 19 \end{pmatrix}$$

Starting with $(1, 0, 0, 1)$, one could generate all Pythagorean 4-tuples with A_4 (and sign changes). In Figure 15, we use the horizontal line to represent a sign change and the vertical line to represent an A_4 transformation. Notice that ${A_4}^2 = Id$.

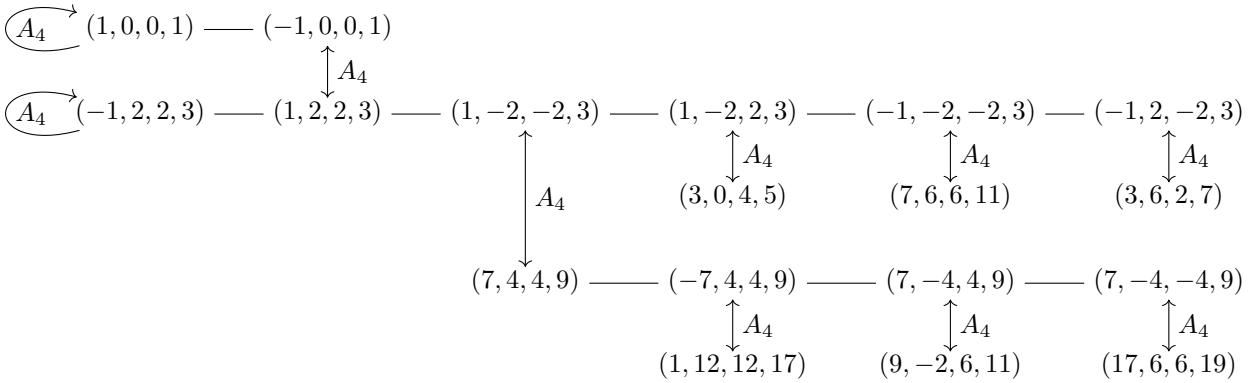

Figure 15: Pythagorean graph (partial)

6.2 Connection to hexagon configuration

For one hexagon primitive integer configuration $(\theta_1, \theta_2, \cdots, \theta_6)$, there are two ways we could generate primitive Pythagorean 4-tuples while maintaining the relative order: $(\theta_1, \theta_3, \theta_5, r_{odd})$ and $(\theta_2, \theta_4, \theta_6, r_{even})$, where

$$r_{odd} = \theta_1 + \theta_2 + \theta_3 = \sqrt{\theta_1^2 + \theta_3^2 + \theta_5^2}$$
$$r_{even} = \theta_2 + \theta_3 + \theta_4 = \sqrt{\theta_2^2 + \theta_4^2 + \theta_6^2}$$

$$(\theta_1, \theta_3, \theta_5, r_{odd}) \quad \leftrightarrow \quad \begin{matrix} r_{odd}-\theta_1-\theta_3 & & \theta_1 \\ & \theta_3 \hexagon r_{odd}-\theta_1-\theta_5 & \\ r_{odd}-\theta_3-\theta_5 & & \theta_5 \end{matrix} \tag{9}$$

$$(\theta_2, \theta_4, \theta_6, r_{even}) \quad \leftrightarrow \quad \begin{matrix} & \theta_2 & r_{even}-\theta_6-\theta_2 \\ r_{even}-\theta_4-\theta_2 & \hexagon & \theta_6 \\ & \theta_4 & r_{even}-\theta_4-\theta_6 \end{matrix} \tag{10}$$

The Pythagorean 4-tuples in (9) and (10) are connected by matrix A_4,

$$\begin{pmatrix} 0 & -1 & -1 & 1 \\ -1 & 0 & -1 & 1 \\ -1 & -1 & 0 & 1 \\ -1 & -1 & -1 & 2 \end{pmatrix} \begin{pmatrix} \theta_1 \\ \theta_3 \\ \theta_5 \\ r_{odd} \end{pmatrix} = \begin{pmatrix} \theta_2 \\ \theta_4 \\ \theta_6 \\ r_{even} \end{pmatrix}$$

More explicitly, one primitive Pythagorean 4-tuple could determine a hexagon in two ways, being mapped to odd fold angles or to even fold angles.

Now we only consider odd-fold representations. Then there is a bijective map from primitive Pythagorean 4-tuples to hexagon primitive integer configurations.

For a pythagorean 4-tuple (a, b, c, r), we define the corresponding hexagon configuration as

$$(\theta_1 = a, \theta_2 = r-a-b, \theta_3 = b, \theta_4 = r-b-c, \theta_5 = c, \theta_6 = r-a-c).$$

Multiplying (a, b, c, r) with A_4, we have another Pythagorean 4-tuple

$$(r-b-c, r-a-c, r-a-b, 2r-a-b-c),$$

which is associated to a configuration rotated 180 degree away from the first configuration.

6.2.1 Sign change, A_4, and flip operations

The inter-set relation for primitive integer hexagon configurations is described by flip operations. With one-to-one correspondence for the set of primitive Pythagorean 4-tuples and primitive integer hexagon configurations, we want to ask whether the inter-set operations of those two sets could be connected in some way.

Definition 6. *For a primitive Pythagorean 4-tuple $x = (x_1, x_2, x_3, x_4)$, a sign change operation S_i a map from $\mathbb{Z}^4$ to $\mathbb{Z}^4$. where $S_i(x)$ only differs x at the sign of the i^{th} element, $i = 1, 2, 3$.*

$$\begin{matrix} (\theta_1, \theta_3, \theta_5, r_{odd}) & \leftrightarrow & \begin{matrix} & \theta_1 & \\ \theta_3 & \hexagon & \\ & \theta_5 & \end{matrix} \\ \Big\downarrow S_1 & & \Big\downarrow F_1 \\ (-\theta_1, \theta_3, \theta_5, r_{odd}) & \leftrightarrow & \begin{matrix} & -\theta_1 & \\ \theta_3 & \hexagon & \\ & \theta_5 & \end{matrix} \end{matrix}$$

Figure 16: Correspondence between the sign change operation and the flip operation

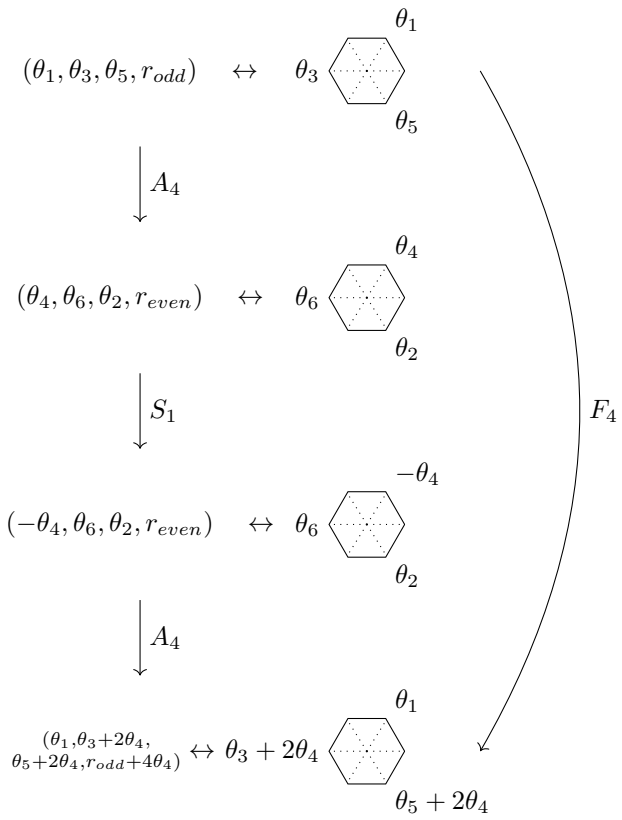

Figure 17: Operations correspondence between Pythagorean 4-tuple and hexagon configuration

As shown in Figure 16, when we apply a sign change S_k on the Pythagorean 4-tuple, we have a corresponding flip operation F_{2k-1} on the hexagon configuration with odd folds θ_1, θ_3, or θ_5.

As shown in Figure 17, the composition of $A_4 \circ S_k \circ A_4$ on Pythagorean 4-tuples, corresponds to flipping an even-indexed fold on hexagon configurations, i.e. one of θ_2, θ_4, or θ_6.

More precisely, the operations on two sets admit the following relations:

$$S_k \leftrightarrow F_{2k-1} \tag{11}$$

$$A_4 \circ S_k \circ A_4 \leftrightarrow F_{2k+2} \tag{12}$$

All the subscripts calculation is under $\mathbb{Z}/6\mathbb{Z}$.

Recall the bijective map derived from the flip graph $\mathcal{G}$ in Theorem 3. This one-to-one correspondence from vertices in $\mathcal{G}$ to primitive integer configurations helps reveal the structure of Pythagorean 4-tuples.

Claim 9. *Every primitive Pythagorean 4-tuple $x = (x_1, x_2, x_3, x_4)$ could be generated by one element of $\mathcal{R}$ through a sequence of sign change and A_4 operations, where*

$$\mathcal{R} = \{(1, 0, 0, 1), (0, 1, 0, 1), (0, 0, 1, 1)\}.$$

Proof. Under odd-fold representations, each primitive Pythagorean 4-tuple x uniquely corresponds to a hexagon configuration. $\mathcal{R}$ with sign change operations S_1, S_2, S_3 uniquely corresponds to six root configurations in the flip graph $\mathcal{G}$.

According to Theorem 3, each primitive integer hexagon configuration could be reached by the root configurations through a sequence of flip operations. The sequence of flip operations has a corresponding sequence of sign change and A_4 operations by Eq 11 and Eq 12. □

6.2.2 Pythagorean graph $\mathcal{H}$ and hexagon flip graph $\mathcal{G}$

To visualize the connection between Pythagorean 4-tuple and hexagon configuration, we define a graph $\mathcal{H}$ reflecting S_i, A_4 operations, and Pythagorean 4-tuples, analogous to the flip graph $\mathcal{G}$

Definition 7 (Restricted graph)**.** *Primitive Pythagorean 4-tuples in $\mathcal{R}$ are three nodes in $\mathcal{H}$.*

If a Pythagorean 4-tuple is generated by the composition of a sequence of S_i and A_4 operations from $\mathcal{R}$, it is denoted as a node in $\mathcal{H}$.

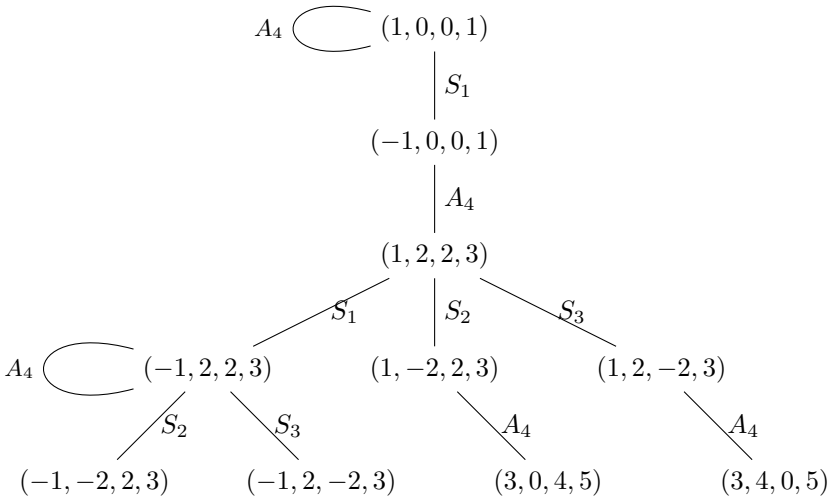

Figure 18: Pythagorean 4-tuple graph $\mathcal{H}$ (partial)

$\mathcal{G}$ and $\mathcal{H}$ (partially shown in Figure 18) have the same number of vertices, since there is a bijection between vertices of $\mathcal{G}$ and vertices of $\mathcal{H}$. This is generated from the bijection between primitive Pythagorean 4-tuples and primitive integer hexagon configurations under the odd-fold representation.

The hexagon flip graph $\mathcal{G}$ and the Pythagorean 4-tuple graph $\mathcal{H}$ can be related by constructing a third graph $\mathcal{K}$, with graph-theoretic maps $\mathcal{K} \to \mathcal{G}$ and $\mathcal{K} \to \mathcal{H}$. The graph $\mathcal{K}$ has twice as many vertices as $\mathcal{G}$ and $\mathcal{H}$, in the sense that $\mathcal{K} \to \mathcal{G}$ and $\mathcal{K} \to \mathcal{H}$ are 2-*to*-1 on vertices.

To get $\mathcal{K}$ from $\mathcal{G}$, $\mathcal{G}$ replaces each vertex with an undirected edge and two vertices.

To get $\mathcal{K}$ from $\mathcal{H}$, $\mathcal{H}$ doubles each vertex and connects two vertices if their parents are connected. This is known as a "double cover" or "degree 2 cover".

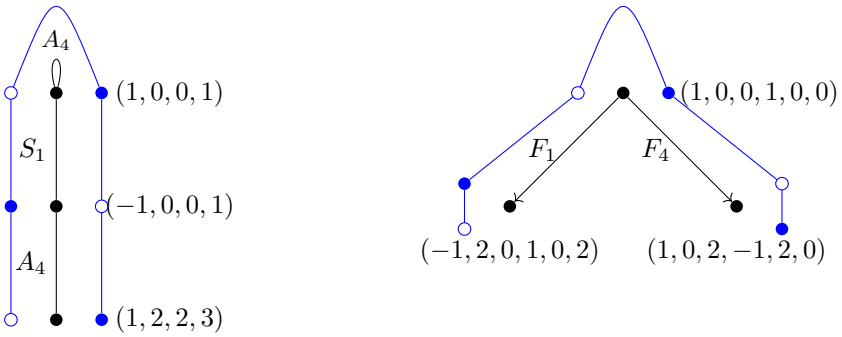

Figure 19: Generate $\mathcal{K}$ from $\mathcal{H}$, generate $\mathcal{K}$ from $\mathcal{G}$

For example, we take Pythagorean 4-tuples

$$(x_1, x_2, x_3, x_4) = (1,0,0,1), (-1,0,0,1), (1,2,2,3),$$

and their corresponding hexagon configurations

$$(\theta_1, \theta_2, \cdots, \theta_6) = (1,0,0,1,0,0), (-1,2,0,1,0,2), (1,0,2,-1,2,0).$$

In Figure 19, the blue graph represents $\mathcal{K}$ partially. The left figure depicts how $\mathcal{H}$ doubles its vertices and recreates corresponding edges, where the transformation formally refers to a "double cover". The right figure depicts how $\mathcal{G}$ replaces a vertex with an undirected edge and two vertices on its ends.

7 Further questions

For the near-flat origami hexagon configuration space, we have investigated points in $\mathbb{R}^6, \mathbb{Z}^6$ on the surface. A natural question followed is how points in $(\mathbb{Z}/k\mathbb{Z})^6$ live in the deformations. Is there any combinatorial structure which is influenced by k? Taking k as a prime, what counting relations could be revealed? How much does the solution subspaces relate to numerical connections? To answer those questions, further studies are needed.

References

[1] D. J. Balkcom and M. T. Mason, *Robotic origami folding*, The International Journal of Robotics Research, 27 (2008), pp. 613–627.

[2] N. Calkin and H. S. Wilf, *Recounting the rationals*, The American Mathematical Monthly, 107(4) (2000), pp. 360–363.

[3] D. Cass and P. J. Arpaia, *Matrix generation of pythagorean n-tuples*, Proceedings of the American Mathematical Society, 109 (1990), pp. 1–7.

[4] B. G.-g. Chen and C. D. Santangelo, *Branches of triangulated origami near the unfolded state*, Physical Review X, 8 (2018), p. 011034.

[5] A. Cuza, Y. Liu, and O. Saeed, *Origami on lattices*, (2019).

[6] G. Darboux, *De l'emploi des fonctions elliptiques dans la théorie du quadrilatère plan*, Bulletin des Sciences Mathématiques et Astronomiques, 2e série, 3 (1879), pp. 109–128.

[7] L. L. Howell, R. J. Lang, M. Frecker, and R. J. Wood, *Special issue: Folding-based mechanisms and robotics*, J. Mechanisms Robotics, 8(3) (2016), p. 030301.

[8] I. Izmestiev, *Four-bar linkages, elliptic functions, and flexible polyhedra*, Computer Aided Geometric Design, 79 (2020), p. 101870.